Novel *p*-Dopant Toward Highly Efficient and Stable Perovskite Solar Cells

Ji-Youn Seo[1†], Hui-Seon Kim[2†*], Seckin Akin[1,3], Marko Stojanovic[1], Elfriede Simon[4], Maximilian Fleischer[4], Anders Hagfeldt[2], Shaik M. Zakeeruddin[1] and Michael Grätzel[1*]

[1]Laboratory for Photonics and Interfaces, Institute of Chemical Sciences and Engineering, School of Basic Sciences, Ecole Polytechnique Fédérale de Lausanne, CH-1015 Lausanne, Switzerland.

[2]Laboratory of Photomolecular Science, Institute of Chemical Sciences and Engineering, School of Basic Sciences, Ecole Polytechnique Fédérale de Lausanne, CH-1015 Lausanne, Switzerland.

[3]Department of Metallurgical and Materials Engineering, Karamanoglu Mehmetbey University, Karaman, Turkey.

[4]Research in Energy and Electronics, Corporate Technology, Siemens AG, 81739 München, Deutschland.

† Both authors contributed equally to this work.

* Corresponding authors

H.-S.K.: hui-seon.kim@epfl.ch and M. G.: michael.graetzel@epfl.ch

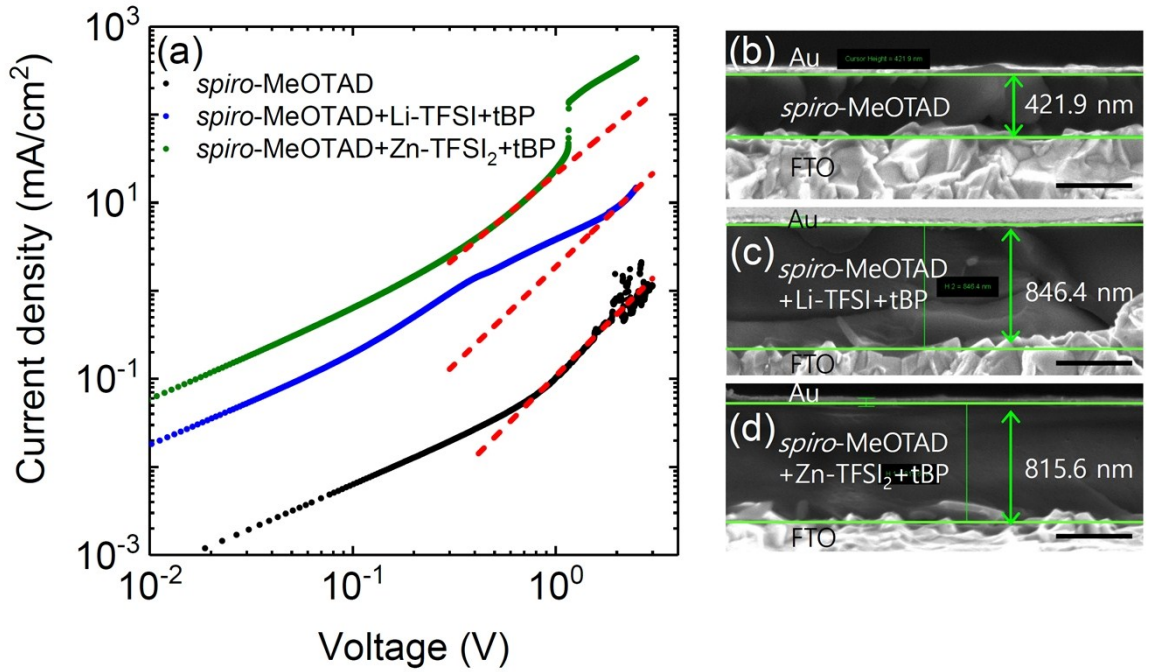

Figure S1 (a) Current (J)-voltage (V) plot of hole only devices. Cross-sectional SEM images of the hole only devices employing (b) *spiro*-MeOTAD, (c) *spiro*-MeOTAD with Li-TFSI and tBP, and (d) *spiro*-MeOTAD with Zn-$TFSI_2$ and tBP. Scale bars in (b)-(d) represent 500 nm.

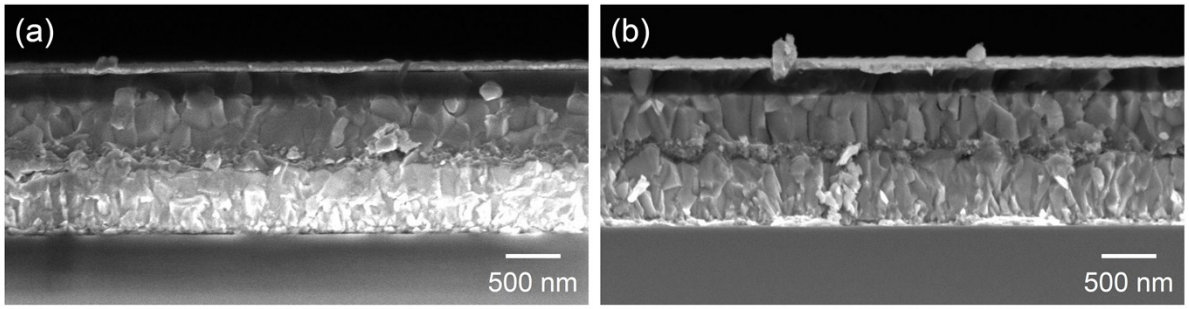

Figure S2 Cross-sectional scanning electron microscope (SEM) images of devices employing (a) Li-TFSI and (b) Zn-$TFSI_2$ as a dopant for *spiro*-MeOTAD.

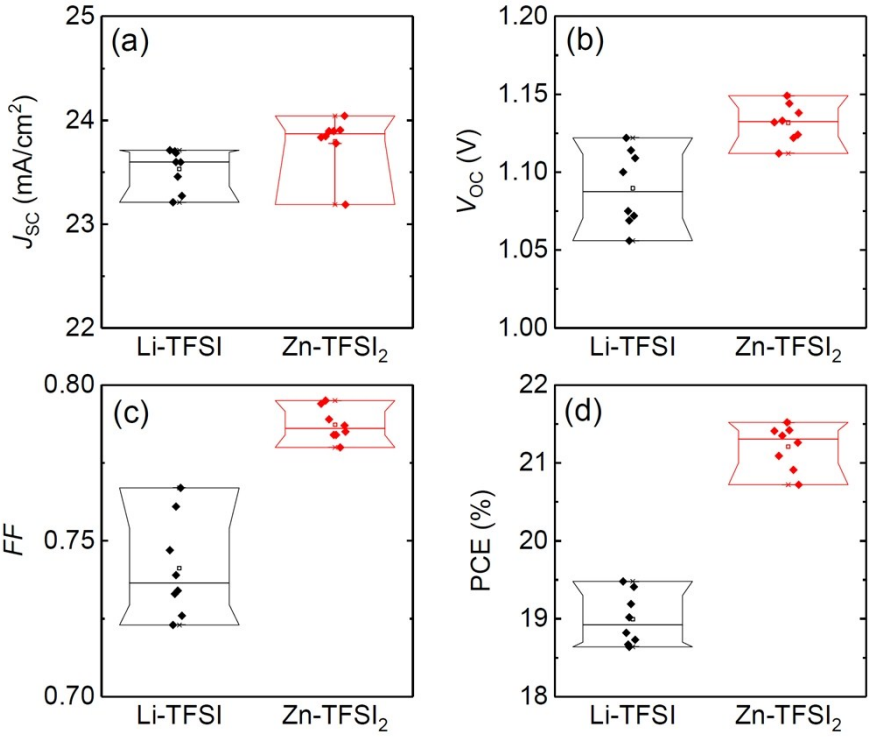

Figure S3 Statistical box charts for the photovoltaic parameters ((a) J_{SC}, (b) V_{OC}, (c) *FF* and (d) PCE) of the devices with respect to the dopant of *spiro*-MeOTAD (black for *spiro*-MeOTAD with Li-TFSI and tBP and red for *spiro*-MeOTAD with Zn-TFSI$_2$ and tBP). V_d=400 ms.

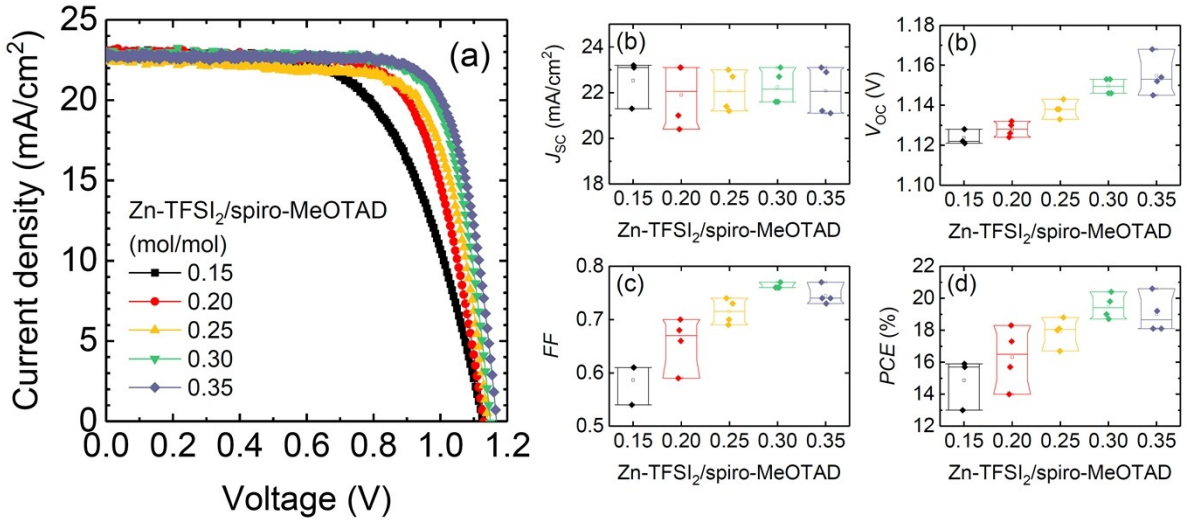

Figure S4 (a) I-V curves of the devices depending on the concentration of Zn-TFSI$_2$ in comparison to the *spiro*-MeOTAD. Statistical box charts of (b) J_{SC}, (c) V_{OC}, (d) *FF* and (e) PCE as a function of the concentration of Zn-TFSI$_2$. The additives of tBP and FK209 were also included in the *spiro*-MeOTAD layer. V_d=500 ms.

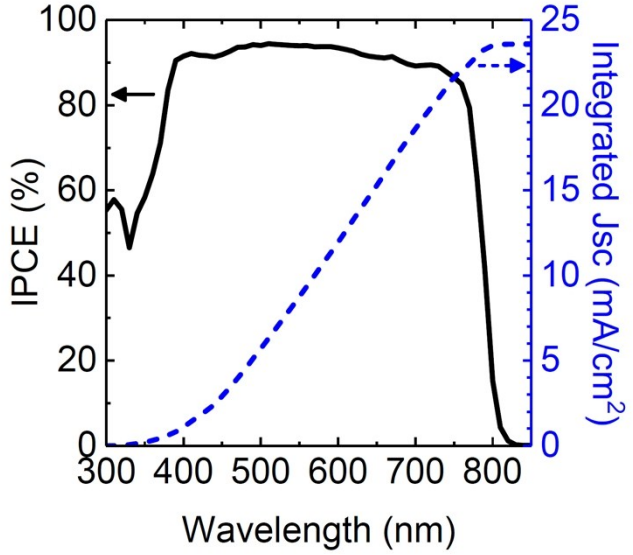

Figure S5 IPCE spectra of the best efficiency device with Zn-$TFSI_2$ in the presence of FK209.

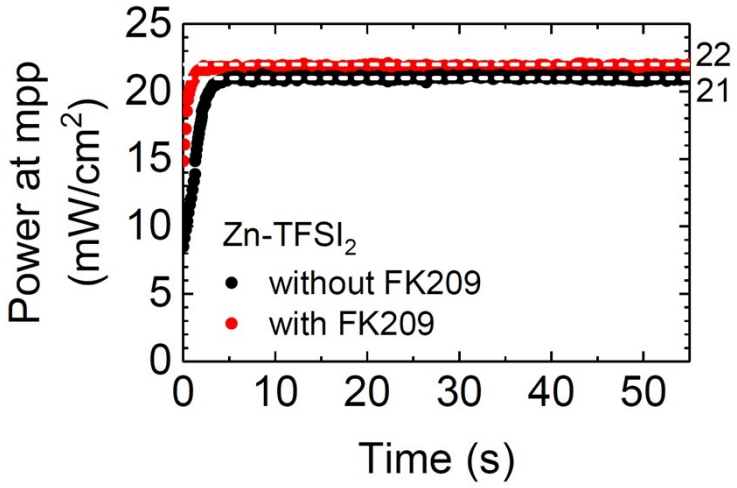

Figure S6 Stabilized power output of devices based on Zn-$TFSI_2$ with respect to the inclusion of FK209.

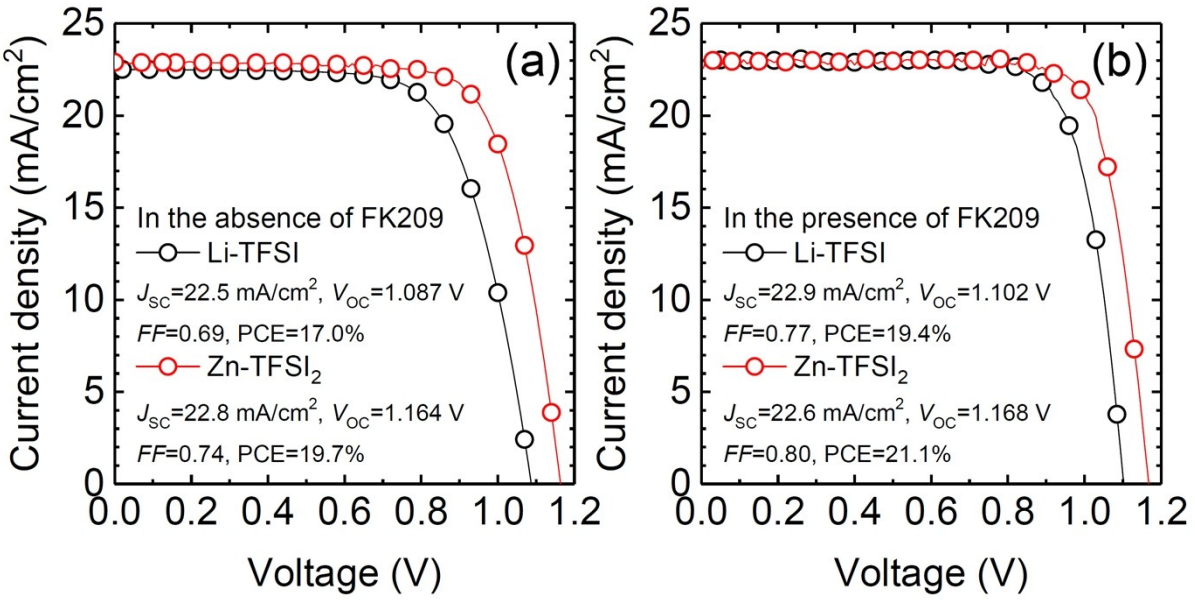

Figure S7 I-V curves of devices based on Li-TFSI or Zn-TFSI$_2$ (a) in the absence of FK209 or (b) in the presence of FK209. The I-V curves were recorded in RS. V_d=500 ms. The devices were prepared and measured in a same manner for comparison. [TFSI$^-$]/[*spiro*-MeOTAD]=0.5 mol/mol.

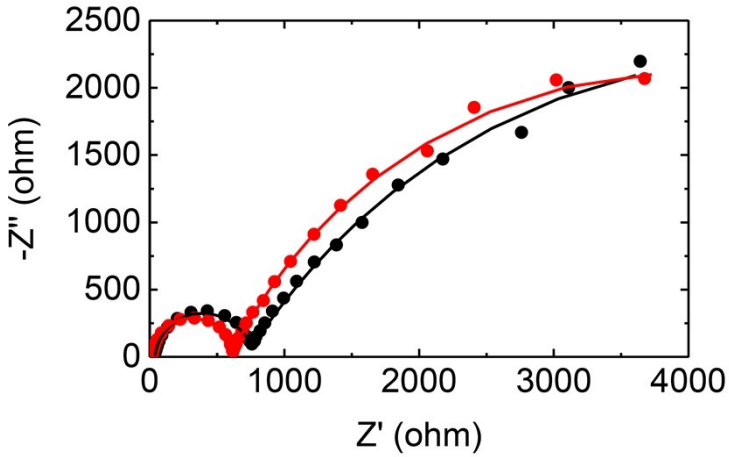

Figure S8 Nyquist plots (dots) and fitting curves (line) (V_{app}=0.0 V) of the devices with Li-TFSI (black) and Zn-TFSI$_2$ (red) as a dopant for *spiro*-MeOTAD.

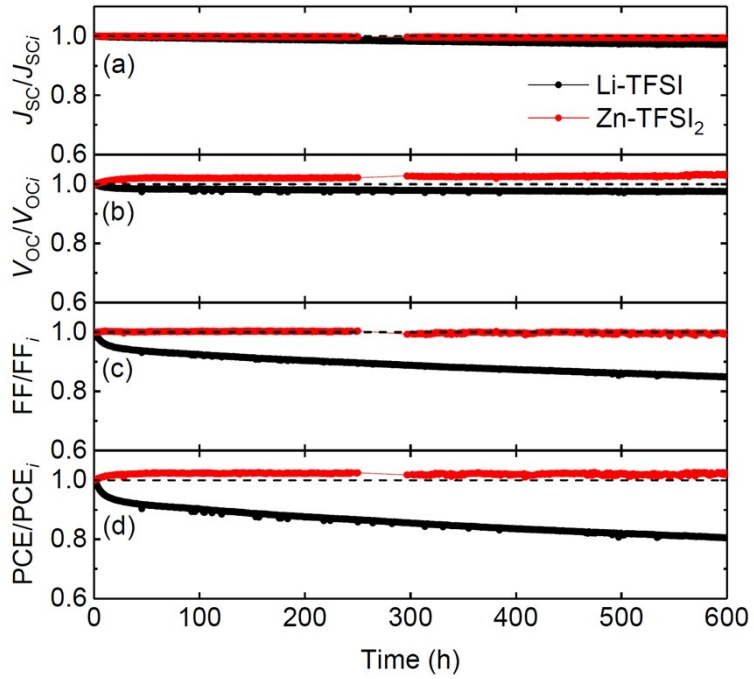

Figure S9 Long-term stability of photovoltaic parameters, (a) J_{SC}, (b) V_{OC}, (c) *FF* and (d) PCE, under one sun at 25 °C with respect to the dopant for the *spiro*-MeOTAD in the presence of FK209. Black and red represent Li-TFSI and Zn-$TFSI_2$. The devices were maintained at the maximum power point (mpp) under the N_2 atmosphere. The initial values of the device with Li-TFSI were 24.3 mA/cm^2 of J_{SCi}, 1.126 V of V_{OCi}, 0.74 of FF_i and 20.2% of PCE_i under 0.998 Sun. The initial values of the device with Zn-$TFSI_2$ were 21.7 mA/cm^2 of J_{SCi}, 1.082 V of V_{OCi}, 0.73 of FF_i and 17.2% of PCE_i under 0.998 Sun.

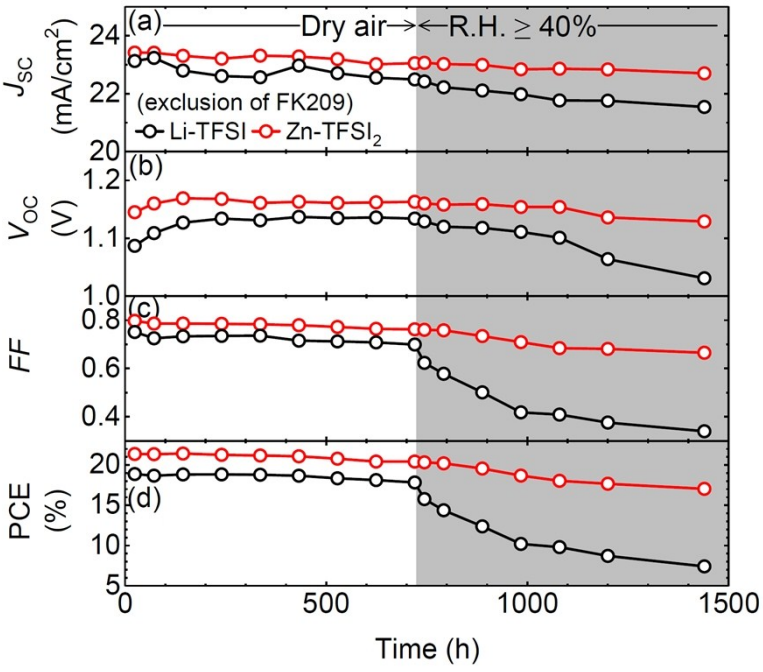

Figure S10 Shelf stability of device employing Li-TFSI or Zn-$TFSI_2$ in the absence of FK209. The device was stored in dark at room temperature. Photovoltaic parameters of (a) J_{SC}, (b) V_{OC}, (c) *FF* and (d) PCE obtained from RS (V_d=400 ms).

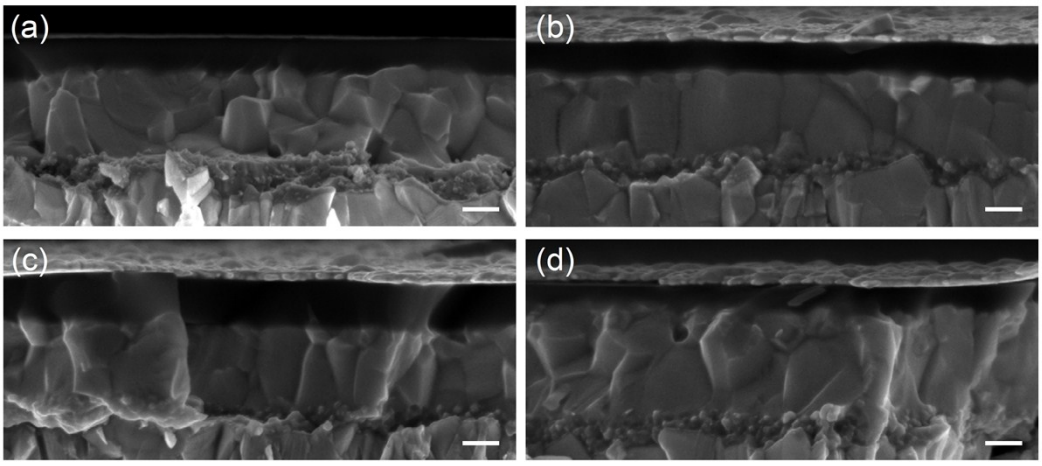

Figure S11 Cross-sectional scanning electron microscope (SEM) images of devices after long-term stability measurements at mpp under one sun and N_2 atmosphere. Device with (a) Li-TFSI and (b) Zn-$TFSI_2$ after 600 h at 25 °C. Device with (c) Li-TFSI and (d) Zn-$TFSI_2$ after 100 h at 50 °C. Scale bars represent 200 nm.

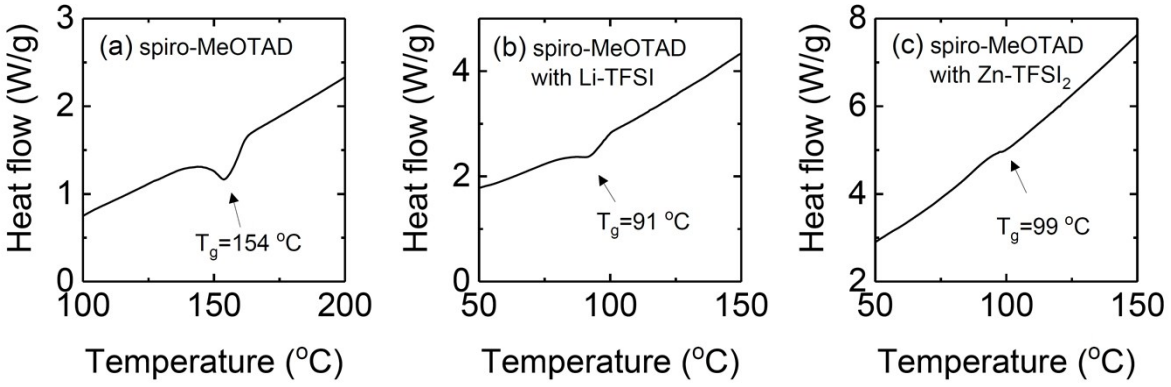

Figure S12 Differential scanning calorimetry (DSC) curves of (a) pristine *spiro*-MeOTAD, (b) *spiro*-MeOTAD with Li-TFSI, FK209 and tBP, and (c) *spiro*-MeOTAD with Zn-$TFSI_2$, FK209 and tBP. The compositional ratio of HTM was exactly same with the one for devices. The DSC curves were obtained from first heating.

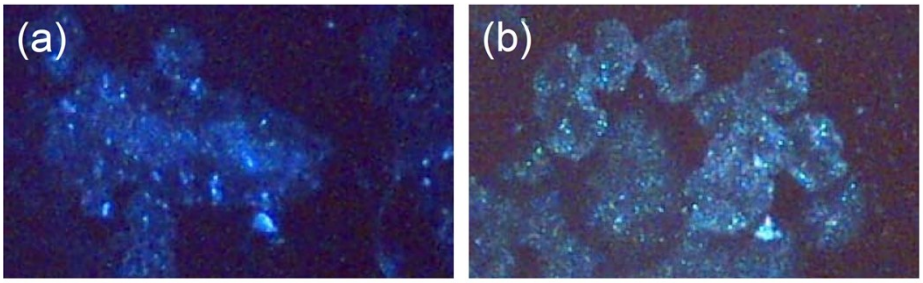

Figure S13 Microscope images (200x magnitude) of *spiro*-MeOTAD with (a) Li-TFSI and (b) Zn-$TFSI_2$ after the thermal stability test for 100 h at 50 °C.

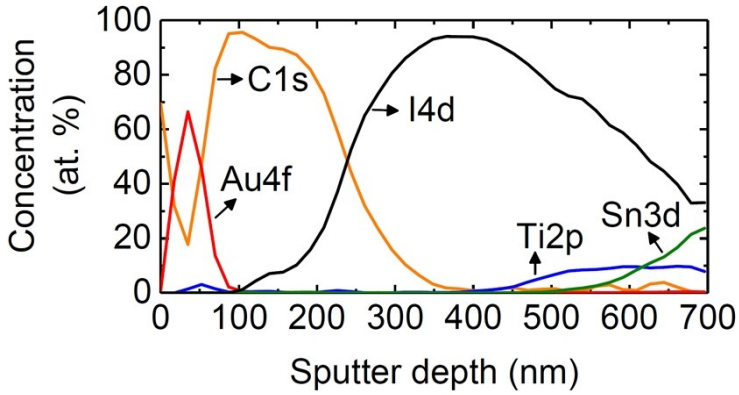

Figure S14 X-ray photoelectron spectroscopy (XPS) depth profiling of the device with Li-TFSI after the thermal stability test for 100 h at 50 °C.